



## Iron oxychloride as an efficient catalyst for selective hydroxylation of benzene to phenol

ElMetwally, Ahmed E.; Eshaq, Ghada; Yehia, Fatma Z.; Al-Sabagh, Ahmed M.; Kegnæs, Søren

*Published in:*  
ACS Catalysis

*Link to article, DOI:*  
[10.1021/acscatal.8b03590](https://doi.org/10.1021/acscatal.8b03590)

*Publication date:*  
2018

*Document Version*  
Peer reviewed version

[Link back to DTU Orbit](#)

### *Citation (APA):*

ElMetwally, A. E., Eshaq, G., Yehia, F. Z., Al-Sabagh, A. M., & Kegnæs, S. (2018). Iron oxychloride as an efficient catalyst for selective hydroxylation of benzene to phenol. *ACS Catalysis*, 8, 10668-10675. <https://doi.org/10.1021/acscatal.8b03590>

---

### General rights

Copyright and moral rights for the publications made accessible in the public portal are retained by the authors and/or other copyright owners and it is a condition of accessing publications that users recognise and abide by the legal requirements associated with these rights.

- Users may download and print one copy of any publication from the public portal for the purpose of private study or research.
- You may not further distribute the material or use it for any profit-making activity or commercial gain
- You may freely distribute the URL identifying the publication in the public portal

If you believe that this document breaches copyright please contact us providing details, and we will remove access to the work immediately and investigate your claim.

## Iron oxychloride as an efficient catalyst for selective hydroxylation of benzene to phenol

Ahmed E. ElMetwally, Ghada Eshaq, Fatma Z. Yehia, Ahmed M. Al-Sabagh, and Søren Kegnæs

*ACS Catal.*, Just Accepted Manuscript • DOI: 10.1021/acscatal.8b03590 • Publication Date (Web): 09 Oct 2018

Downloaded from <http://pubs.acs.org> on October 15, 2018

### Just Accepted

“Just Accepted” manuscripts have been peer-reviewed and accepted for publication. They are posted online prior to technical editing, formatting for publication and author proofing. The American Chemical Society provides “Just Accepted” as a service to the research community to expedite the dissemination of scientific material as soon as possible after acceptance. “Just Accepted” manuscripts appear in full in PDF format accompanied by an HTML abstract. “Just Accepted” manuscripts have been fully peer reviewed, but should not be considered the official version of record. They are citable by the Digital Object Identifier (DOI®). “Just Accepted” is an optional service offered to authors. Therefore, the “Just Accepted” Web site may not include all articles that will be published in the journal. After a manuscript is technically edited and formatted, it will be removed from the “Just Accepted” Web site and published as an ASAP article. Note that technical editing may introduce minor changes to the manuscript text and/or graphics which could affect content, and all legal disclaimers and ethical guidelines that apply to the journal pertain. ACS cannot be held responsible for errors or consequences arising from the use of information contained in these “Just Accepted” manuscripts.



# Iron oxychloride as an efficient catalyst for selective hydroxylation of benzene to phenol

Ahmed E. ElMetwally\*,<sup>a</sup>, Ghada Eshaq<sup>a</sup>, Fatma Z. Yehia<sup>a</sup>, Ahmed M. Al-Sabagh<sup>b</sup>, Søren Kegnæs<sup>c</sup>

<sup>a</sup> *Petrochemicals department, Egyptian Petroleum Research Institute, Nasr City, Cairo 11727, Egypt*

<sup>b</sup> *Petroleum applications department, Egyptian Petroleum Research Institute, Nasr City, Cairo 11727, Egypt*

<sup>c</sup> *DTU Chemistry, Technical University of Denmark, Kemitorvet 207, DK-2800 Kgs. Lyngby, Denmark*

## ABSTRACT

Selective hydroxylation of benzene is a felicitous strategy for the production of phenol that is deemed an alternative route for conventional processes. Thus, the development of a durable and highly efficient catalyst for the selective hydroxylation of benzene should be the key topic. In this work, FeOCl was prepared by chemical vapor transition method and characterized using various techniques including XRD, TEM, Raman spectroscopy, N<sub>2</sub> adsorption–desorption, DLS and TGA. The prepared FeOCl was applied as heterogeneous catalyst in benzene hydroxylation and the reaction conditions were optimized. The acquired data manifested that FeOCl has shown superiority over the other reported catalysts utilized in benzene hydroxylation. The superiority of FeOCl is attributed to the facile self-redox potential of FeOCl and its remarkable ability for the production of an overwhelming amount of hydroxyl radicals in a short period of time. The catalyst recovery and reusing test showed that FeOCl is able to endure the harsh conditions of benzene hydroxylation for four runs. The mechanism of benzene hydroxylation using FeOCl as a catalyst in the presence of hydrogen peroxide as an oxidant was also illustrated.

**Keywords:** benzene; phenol; hydroxylation; catalysis; oxychloride

\*corresponding author: Tel: +201115025588, Fax: +20222747433

E-mail address: [ahmed\\_ezzatt@msn.com](mailto:ahmed_ezzatt@msn.com)

## INTRODUCTION

Phenol is deemed as one of the most indispensable organic compound that is used extensively in various chemical and petrochemical industries. Phenol is also used as an intermediate in the production of phenol derivatives and phenolic resins. Cumene process is commonly used for the production of nearly 90% of phenol produced throughout the globe, where propylene and benzene are used as starting materials with acetone as a side product.<sup>1-2</sup> Cumene process comprises three consecutive stages and suffers from various drawbacks including excessive energy consumption and the generation of hazardous intermediate such as cumene hydroperoxide. In spite of the economic importance for the production of acetone, the demand for phenol is still rising as the global demand for phenol is currently being driven by an increasing demand of its various derivatives.<sup>1, 3</sup> Consequently, the production of phenol from the direct oxidation of benzene has attracted much attention to overcome the drawbacks encountered with cumene process.<sup>4-6</sup>

Recently, great efforts have been made to develop the catalytic system of the direct oxidation of benzene to phenol especially when the hydrogen peroxide is used as an oxidant.<sup>7</sup> During this tenure, several catalysts including palladium membrane, modified titanium silicalite, titanium-mesoporous molecular sieves, vanadium-substituted polyoxometalates, activated carbon, cerium promoted V-g-C<sub>3</sub>N<sub>4</sub> and vanadium-containing mesoporous carbon have been explored.<sup>8-22</sup> Among these explored catalysts, iron-based catalysts have shown supremacy over the other tested catalysts in different aspects including the cost, abundance, environmental friendliness and low toxicity.

1  
2  
3 Previous studies reported that iron-based catalysts were highly efficient and selective when  
4 used as catalysts in different oxidative processes and particularly the challenging processes.<sup>23-25</sup>  
5  
6 Wang et al.<sup>26</sup> reported that a high phenol yield from benzene hydroxylation can be achieved over  
7  
8 two Fe-based metal–organic frameworks catalysts using hydrogen peroxide as an oxidant.  
9  
10 Jourshabani et al.<sup>27</sup> studied the effect of using Fe-supported cage like mesoporous silica in benzene  
11  
12 hydroxylation to phenol using H<sub>2</sub>O<sub>2</sub> as an oxidant. Baykan and Oztas,<sup>28</sup> reported the synthesis of  
13  
14 phenol via the direct hydroxylation of benzene over iron phosphate. Carneiro and Silva,<sup>29</sup> studied  
15  
16 the direct hydroxylation of benzene to phenol using hydrogen peroxide in the presence of Fe(III)  
17  
18 Schiff base complex as a catalyst. Recently, iron ferrite was reported to be an efficient catalyst for  
19  
20 the selective hydroxylation of benzene to phenol under mild conditions in the presence of hydrogen  
21  
22 peroxide as an oxidant.<sup>30</sup> Although the examined catalysts were efficient and selective in benzene  
23  
24 hydroxylation, the phenol yield did not reach its climax as this process still demand more  
25  
26 development. Thus, exploring a catalyst that is able to enhance the phenol yield remains a major  
27  
28 goal. Such catalyst will be able to minimize the production of different byproducts while  
29  
30 maintaining a high phenol yield.  
31  
32  
33  
34  
35  
36  
37

38 Iron oxychloride (FeOCl) is a ternary layered material that have distinguished layered  
39  
40 framework and unrivaled chemical stability. The layers of this distinguishable layered framework  
41  
42 are attached together by van der Waals interaction, which makes FeOCl able to host organic  
43  
44 compounds.<sup>31</sup> The charge transfers between the host organic compound and FeOCl may change  
45  
46 iron oxidation state from +3 to +2.<sup>32</sup> Studies revealed that hosting an organic compound within  
47  
48 FeOCl layered framework was responsible for the in situ reduction of one fourth of Fe<sup>3+</sup> to Fe<sup>2+</sup>.<sup>32-</sup>  
49  
50  
51  
52  
53  
54  
55  
56  
57  
58  
59  
60  
<sup>33</sup> FeOCl has been employed as a catalyst in the degradation of some persistent organic compound

1  
2  
3 and found to have fabulous activity, which is attributed to the extraordinary structural  
4 configuration of its atoms and also for its reducible electronic characteristics.<sup>34</sup>  
5  
6  
7

8 We believe that this is the first article that uses FeOCl as a heterogeneous catalyst in benzene  
9 hydroxylation to phenol. Herein, FeOCl was prepared using chemical vapor transition method and  
10 characterized using XRD, TEM, Raman spectroscopy, N<sub>2</sub>- sorption, DLS and TGA analysis.  
11 FeOCl was examined in benzene hydroxylation and the reaction conditions were optimized to  
12 fulfil the maximum phenol yield. Finally, the reaction mechanism of benzene hydroxylation using  
13 FeOCl was illustrated.  
14  
15  
16  
17  
18  
19  
20  
21  
22

## 23 **EXPERIMENTAL**

### 24 **Materials**

25  
26  
27  
28 Anhydrous iron (III) chloride and ethylene glycol were supplied from Sigma–Aldrich. Benzene  
29 and ammonia solution (30%) were supplied from Merck. Hydrogen Peroxide (30 %) was supplied  
30 from PanReac AppliChem. Acetic Acid (70-80% w/w) was supplied from Fisher Scientific.  
31  
32  
33  
34  
35

### 36 **Preparation of FeOCl**

37  
38 First,  $\alpha$ -Fe<sub>2</sub>O<sub>3</sub> was prepared by dissolving certain amount of anhydrous ferric chloride in  
39 aqueous solution containing 80% ethylene glycol. Ferric ions were precipitated by adding 3 M  
40 ammonia solution under stirring at 50°C and kept at this temperature for 30 min. The formed slurry  
41 was aged for 12 h and then the resultant precipitate was separated by centrifugation, washed by  
42 deionized water and dried at 100°C overnight. Second, FeOCl was prepared by chemical vapor  
43 transition method from the prepared Fe<sub>2</sub>O<sub>3</sub> according to the procedure reported in.<sup>34</sup> In particular,  
44 the prepared  $\alpha$ -Fe<sub>2</sub>O<sub>3</sub> was mixed with anhydrous ferric chloride in ratio of 1:1.3. The resultant  
45 mixture was sealed in an evacuated glass vessel and kept in a muffle furnace for 48 h at 380°C.  
46  
47  
48  
49  
50  
51  
52  
53  
54  
55  
56  
57

1  
2  
3 The obtained sample was washed successively with acetone to get rid of the unreacted ferric  
4 chloride and eventually dried at 100 °C for 6 h.  
5  
6  
7

### 8 9 **Characterization**

10  
11 A JEOL JEM-2100 operating at 200 kV was used to obtain the TEM images of the sample.  
12  
13

14 The hydrodynamic diameter was characterized using dynamic light scattering (DLS) analysis  
15 on a Malvern Zetasizer Nano (Malvern Instruments Ltd., Worcestershire, UK). XRD analysis was  
16 performed to identify and confirm the phase of the prepared sample using a Philips powder  
17 diffractometer using Cu K $\alpha$  radiation. The analysis was carried out at a scanning speed of 2°  $\theta$ /min  
18 and 2 $\theta$  step of 0.02°. The Raman spectra of the prepared sample was obtained using a Bruker  
19 Optics Raman spectrometer operating at room temperature with an exciting lines of 532 nm. TGA  
20 analysis was conducted at rate of 10°C min<sup>-1</sup> under nitrogen atmosphere on a SDT Q600, TA  
21 Instruments. A NOVA 3200 system instrument was used to obtain the surface texture parameters  
22 by nitrogen sorption at -195.85°C.  
23  
24  
25  
26  
27  
28  
29  
30  
31  
32  
33

### 34 **Catalytic activity**

35  
36  
37 The reaction was carried out in a 25 mL two necked flask equipped with a condenser. The  
38 reaction temperature was adjusted by immersing the flask in a thermally controlled oil bath. In  
39 each run, benzene (0.9 mL) and 70% acetic acid (1 mL) were fed into the two necked flask  
40 followed by the addition of a particular amount of FeOCl. Thereafter, certain amount of 30%  
41 hydrogen peroxide was introduced to the reaction medium. The catalytic activity was evaluated  
42 at different reaction temperature in the range of 30-80°C and at different reaction time in the range  
43 of 0.5-6 h. When the reaction was complete, the catalyst was separated by centrifugation and the  
44 liquid product was collected to be analyzed. An Agilent 7890 GC equipped with HP-5 capillary  
45  
46  
47  
48  
49  
50  
51  
52  
53  
54  
55  
56  
57  
58  
59  
60

1  
2  
3 column (5%-Phenyl)-methylpolysiloxane (30 m, 0.25  $\mu\text{m}$  and 0.32 mm) and flame ionization  
4  
5 detector. The phenol selectivity was obtained as the molar ratio of the produced phenol to the  
6  
7 converted benzene while the phenol yield was obtained as the molar ratio of the produced phenol  
8  
9 to the initial benzene. *p*-benzoquinone selectivity was obtained as the molar ratio of the produced  
10  
11 *p*-benzoquinone to the converted benzene.<sup>35</sup>  
12  
13

## 14 15 **Results and Discussion**

### 16 17 **Catalyst characterization**

18  
19  
20  
21 The TEM micrograph of the prepared sample reveals that catalyst has a stone-like  
22  
23 morphology with a size in the range of 40–50 nm as displayed in Figure 1.  
24

25  
26 Dynamic light scattering technique was conducted to screen the size distribution of the  
27  
28 prepared FeOCl. The obtained data reveal that the diameter range of FeOCl is 50 nm as displayed  
29  
30 in Figure 1.  
31

32  
33 The phase of the prepared FeOCl sample was identified and confirmed using the obtained  
34  
35 XRD pattern presented in Figure 1. The phase of the prepared FeOCl is confirmed by matching  
36  
37 the obtained pattern with the FeOCl reference code (01-072-0619). The obtained data manifest  
38  
39 that the prepared FeOCl has an orthorhombic structure with a crystallite size of 50 nm that was  
40  
41 calculated using Scherrer equation, which is in consistence with the data observed in the TEM  
42  
43 micrograph and DLS analysis.  
44

45  
46 The Raman spectrum of the prepared FeOCl (Figure 1) exhibits band at 216  $\text{cm}^{-1}$  that can be  
47  
48 ascribed to Fe–Cl stretching modes while the bands appear at 285  $\text{cm}^{-1}$  and 400  $\text{cm}^{-1}$  can be  
49  
50 ascribed to Fe–O stretching modes.  
51

52  
53 The acquired  $\text{N}_2$  sorption isotherm of the prepared FeOCl reveals that the sample can be  
54  
55 categorized to Type II as shown in Figure 1. The isotherm of FeOCl exhibits an initial knee, which  
56  
57



1  
2  
3 is attributed to the monolayer formation. It should be mentioned that the region observed for the  
4  
5 onset of multilayer formation is usually recognized with initial concaved portion followed by a  
6  
7 hoist that ascribed to multilayer formation. It is obvious that the FeOCl isotherm exhibits an H3  
8  
9 hysteresis that extends  $P/P^0 = 0.15$ . These characteristics can be ascribed to the existence of fragile  
10  
11 narrow pores that imploded during the formation of monolayer leading to the formation of an open  
12  
13 texture with a slit shape where a limited numbers of multilayer is formed.<sup>36-37</sup> The value of specific  
14  
15 surface area calculated using BET equation for FeOCl is  $17.11 \text{ m}^2\text{g}^{-1}$ , and the total pore volume  
16  
17 ( $V_p$ ) taken at  $P/P_0 = 0.95$ , is  $0.034 \text{ mL g}^{-1}$ . The BJH calculation method was used to obtain the  
18  
19 pore size distribution curves as shown in Figure 1. The pore size distribution curve of iron  
20  
21 oxychloride implies the presence of a sharp peak with a climax centered at  $19 \text{ \AA}$  and broad peak  
22  
23 with a climax centered at  $46 \text{ \AA}$ .

24  
25  
26  
27  
28  
29 The thermal stability analysis was carried out prior to the catalytic testing to make sure the  
30  
31 catalyst is able to endure the reaction temperature of benzene hydroxylation. It also provides a  
32  
33 preliminary survey whether the reusability of the employed catalyst is possible or not. The TGA  
34  
35 analysis of the prepared FeOCl (Figure 1) reveals that the catalyst endures the examined  
36  
37 temperature range without any obvious transformational change. Thus, it can be inferred that the  
38  
39 employed catalyst is thermally stable within the range of the tested reaction temperature of benzene  
40  
41 hydroxylation.  
42  
43  
44  
45  
46  
47  
48  
49  
50  
51  
52  
53  
54  
55  
56  
57  
58  
59  
60

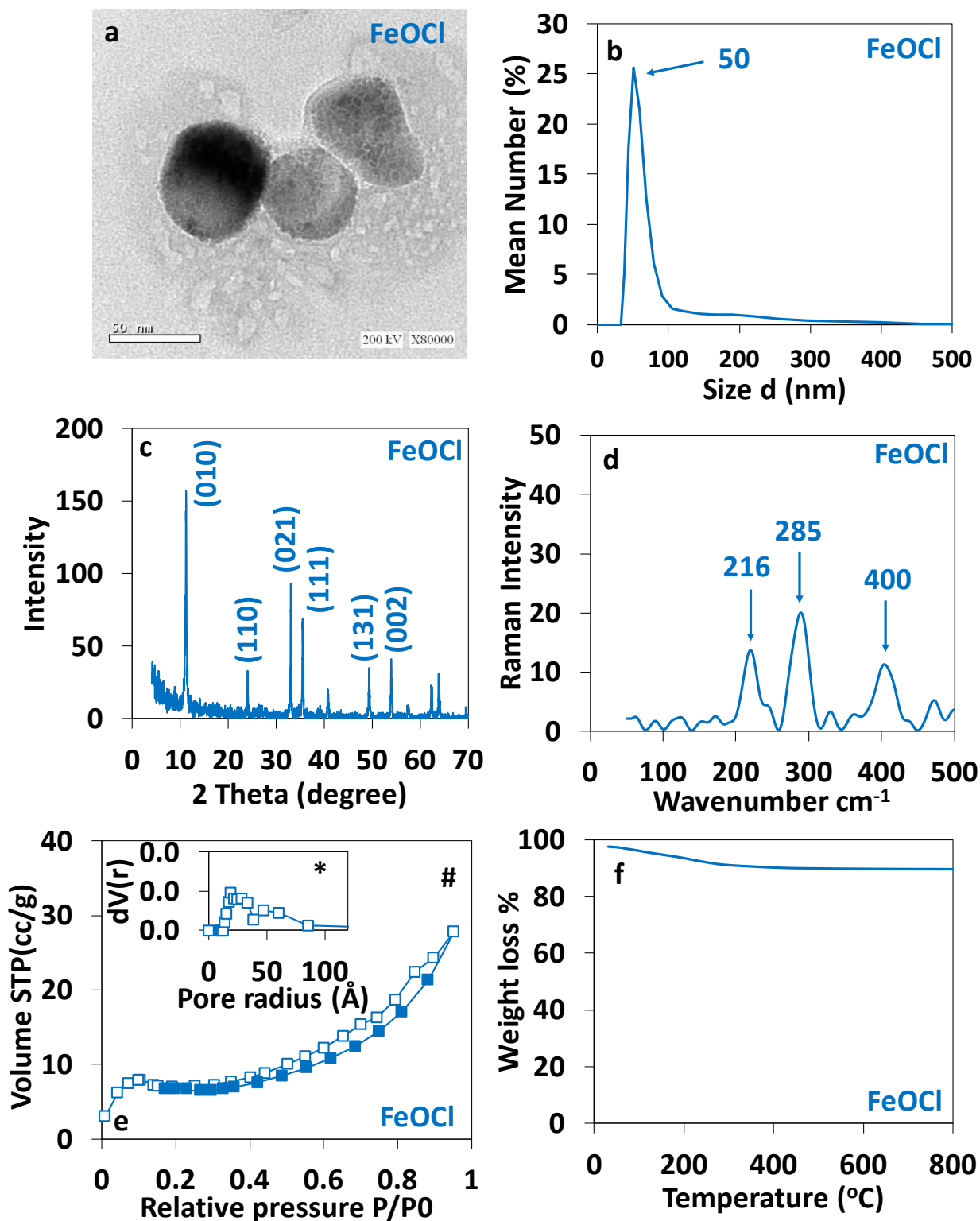


**Figure 1.** (a) TEM image of FeOCl. (b) DLS of FeOCl (c) XRD pattern of FeOCl. (d) Raman spectrum of FeOCl. (e#) N<sub>2</sub> adsorption-desorption isotherm of FeOCl (e\*) pore size distribution curve of FeOCl. (f) TGA curve of FeOCl.

## The catalytic activity of FeOCl in benzene hydroxylation

### Impact of reaction time

The impact of reaction time is a very important parameter that gives us a wide view on the catalytic performance of the catalyst. When the phenol yield becomes steady or decreases this means that either the radical chain reaction is brought to an end or the generated phenol is further oxidized. The impact of reaction time on benzene hydroxylation was tested in the 0.5-6 h range as presented in Figure 2 and Table S1. The obtained data reveal that the phenol yield is directly proportional to the reaction time reaching a climax with a value of 43.5% after 4 h of benzene hydroxylation and beyond this time the phenol yield slightly decreases. Consequently, the use of elongated time of benzene hydroxylation has a negative impact on the phenol yield because the produced phenol undergoes further oxidation. Thus, it can be inferred that beyond 4 h of benzene hydroxylation a significant portion of the generated radical species tends to oxidize the produced phenol molecules instead of attacking benzene molecules. This explanation agrees well with the data obtained for phenol selectivity upon increasing the reaction time, which reveals a slight decrease in the phenol selectivity due to the production of *p*-Benzoquinone (Table S2 and Figure S1) as a side product. *p*-Benzoquinone is a stable side product produced as result of hydroquinone oxidation.

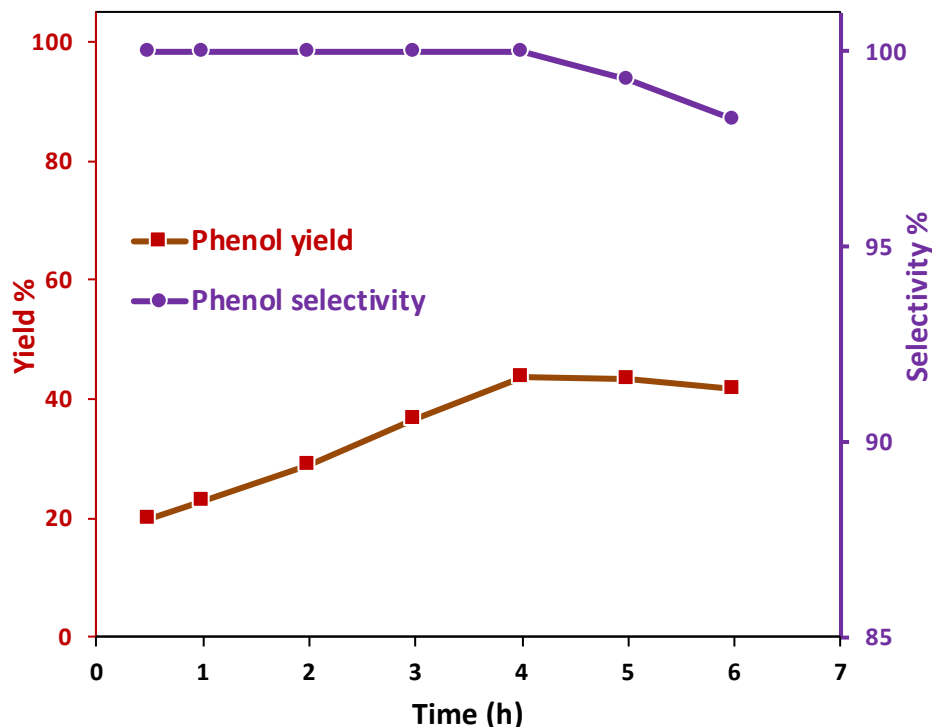


**Figure 2.** Impact of reaction time. Reaction conditions: Benzene (0.9 mL), FeOCl (0.1 g), benzene: H<sub>2</sub>O<sub>2</sub> (1:1), acetic acid (1 mL) and 60°C.

Compared to the previously reported data (Table S3), a maximum phenol yield of 43.5 % in only 4h of benzene hydroxylation highlights the high efficacy of FeOCl. This high efficacy can be attributed to the unique ability of FeOCl for the production of a high amount of hydroxyl radicals in a short period of time. This ability can be ascribed to the substantial structure of FeOCl where its polar surface and specifically the 020 plane is overstuffed with a huge number of unsaturated Fe atoms.<sup>38</sup> Compared to water, the hydrogen peroxide molecules have more affinity to the polarized plan of iron oxychloride.<sup>34</sup> These Fe atoms were uniformly arranged on this plan with a O–Fe–Cl configuration.

1  
2  
3 Compared to  $\alpha$ -FeOOH, FeOCl is able to increase the production of hydroxyl radicals from  
4 hydrogen peroxide with a yield 100 times higher than that produced in the presence of  $\alpha$ -FeOOH.<sup>34</sup>  
5  
6 Moreover, the Fe<sup>3+</sup> ions of the iron oxychloride are susceptible to be reduced to Fe<sup>2+</sup> ions upon  
7 their reaction or intercalation with different species, which makes clear that FeOCl is distinguished  
8 by facile self-redox properties. The Fe<sup>2+</sup> ions are able to catalyze the production of hydroxyl  
9 radicals from hydrogen peroxide with a rate 1000-10000 times higher than that produced in the  
10 presence of Fe<sup>3+</sup> ions.<sup>39</sup> A partial reduction could occur as a result of the electron-charge transition  
11 from hydrogen peroxide to FeOCl upon the adsorption of hydrogen peroxide and organic  
12 molecules over the FeOCl surface.  
13  
14  
15  
16  
17  
18  
19  
20  
21  
22



23  
24  
25  
26  
27  
28  
29  
30  
31 Thus, the efficacy of FeOCl in benzene hydroxylation can be attributed to unique features of FeOCl  
32 and the matchless configuration.  
33  
34  
35

### 36 37 **Impact of catalyst dosage**

38  
39  
40 To find out the most suitable catalyst dosage on phenol yield, benzene hydroxylation  
41 reaction was carried out using different catalyst doses in the 0.05-0.25 g range as displayed in  
42 Figure 3. The results show that the phenol yield increases with increasing the catalyst dosage and  
43 it reaches a maximum value at a catalyst dosage of 0.1 g and beyond this amount the phenol yield  
44 decreases. It is clear that increasing the catalyst dosage has a positive impact on the phenol yield  
45 because of increasing the number of active sites that leads to a massive increase in the amount of  
46 hydroxyl radicals. However, the addition of an excessive amount of catalyst has a negative impact  
47  
48  
49  
50  
51  
52  
53  
54  
55  
56  
57

on the phenol yield because of the agglomeration of the catalyst particles that block the active sites. This blockage prevents the benzene molecules from reaching the active sites that are rich with highly active hydroxyl radicals and consequently the hydroxyl radicals tend to scavenge each other instead of attacking the benzene molecules.

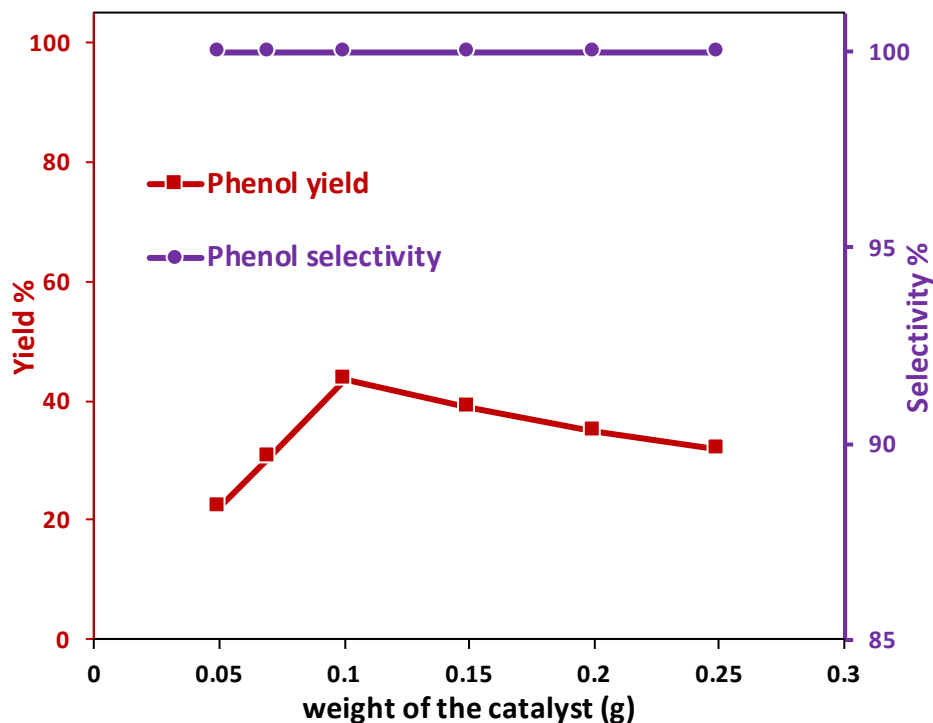


**Figure 3.** Impact of catalyst dosage. Reaction conditions: Benzene (0.9 mL), benzene: H<sub>2</sub>O<sub>2</sub> (1:1), acetic acid (1 mL), 60°C and 4 h.

### Impact of benzene:H<sub>2</sub>O<sub>2</sub> molar ratio

To maximize the yield of phenol using FeOCl as a catalyst, we carefully optimized the benzene to hydrogen peroxide ratio as the addition of an excessive amount of hydrogen peroxide may have a negative impact on the oxidation process. Thus, it is highly recommended to carefully adjust the concentration of hydrogen peroxide to fulfil a maximum phenol yield. The impact of

benzene:H<sub>2</sub>O<sub>2</sub> molar ratio on the hydroxylation of phenol was examined in the range from 1:0.5 to 1:2 as displayed in Figure 4. The obtained results reveal that the phenol yield is directly proportional to the benzene:H<sub>2</sub>O<sub>2</sub> molar ratio, peaking at the molar ratio 1:1 and beyond this ratio the phenol yield declines.

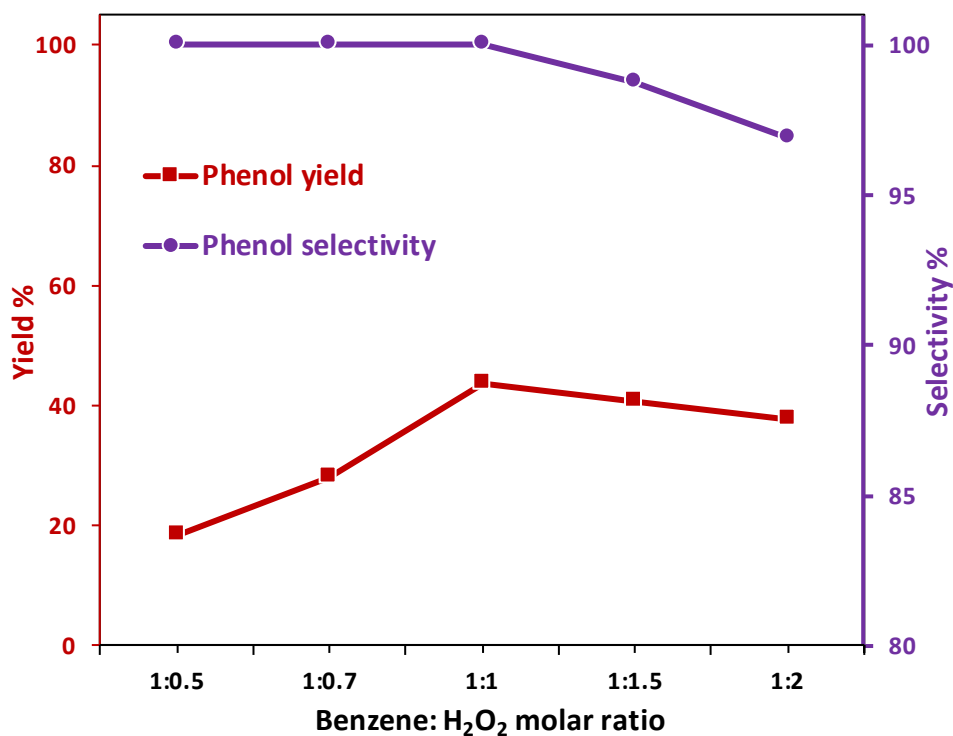


**Figure 4.** Impact of benzene:H<sub>2</sub>O<sub>2</sub> molar ratio. Reaction conditions: Benzene (0.9 mL), FeOCl (0.1 g), acetic acid (1 mL), 60°C and 4h.

It should be noted that the maximum H<sub>2</sub>O<sub>2</sub> efficiency was detected at the molar ratio 1:1 in the presence of FeOCl as a catalyst as presented in Figure S2. The enhancement of the phenol yield upon increasing the benzene:H<sub>2</sub>O<sub>2</sub> molar ratio is attributed to the presence of a considerable

amount of H<sub>2</sub>O<sub>2</sub> that produces higher amounts of hydroxyl radicals. However, the decline of the phenol yield upon the use of higher concentration of hydrogen peroxide is attributed to the presence of an overwhelming amount of H<sub>2</sub>O<sub>2</sub> that scavenges the produced hydroxyl radicals with a rate,  $k = 2.7 \times 10^7 \text{ M}^{-1}\text{s}^{-1}$ . The reaction of H<sub>2</sub>O<sub>2</sub> with hydroxyl radicals gives rise to hydroperoxyl radicals. The generated hydroperoxyl radicals also reacts with hydroxyl radicals ( $k = 6 \times 10^9 \text{ M}^{-1}\text{s}^{-1}$ ) and consequently more hydroxyl radicals will be lost as presented in the following equations.<sup>40-43</sup>



Another explanation of the decline of the phenol yield upon using an excessive concentration of H<sub>2</sub>O<sub>2</sub> is the further of oxidation of the produced phenol to *p*-Benzoquinone. This explanation is supported by the decline of phenol selectivity upon increasing the benzene:H<sub>2</sub>O<sub>2</sub> molar ratio. Thus, the produced radicals are involved in phenol oxidation instead of attacking the benzene molecules.

### Impact of reaction temperature

The impact of reaction temperature on benzene hydroxylation was examined in the 30-80°C range to find out the lowest temperature that provides the maximum phenol yield as displayed in Figure 5. The adjustment of the reaction temperature in a catalytic system that contains hydrogen peroxide as an oxidant is a quite intricate operation. The use of elevated temperature leads to the decomposition of hydrogen peroxide into water and oxygen and consequently a great portion of the hydrogen peroxide will be lost. Screening the reaction temperature reveals that the phenol yield is directly proportional to the reaction reaching its climax at 60°C, and beyond this temperature the phenol yield decreases. It can be argued that increasing the reaction temperature reduces the mass transfer limitation of hydroxyl radicals and thus the rate of the reaction between the benzene molecule and hydroxyl radicals is significantly enhanced. Furthermore, the oxidation rate of the



organic compounds is greatly enhanced upon using elevated temperature.<sup>44</sup> However, the use of excessively elevated temperature such as 80°C has a negative impact on the phenol yield as the hydrogen peroxide is thermally decomposed into oxygen and water.

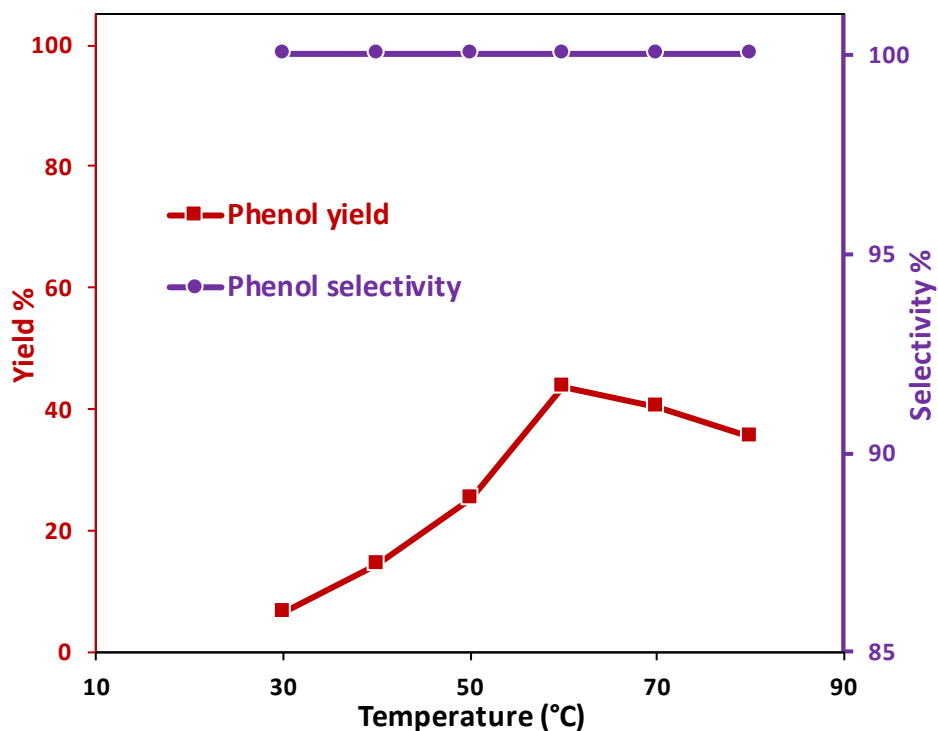


**Figure 5.** Impact of reaction temperature. Reaction conditions: Benzene (0.9 mL), FeOCl (0.1 g), benzene: H<sub>2</sub>O<sub>2</sub> (1:1), acetic acid (1 mL) and 4h.

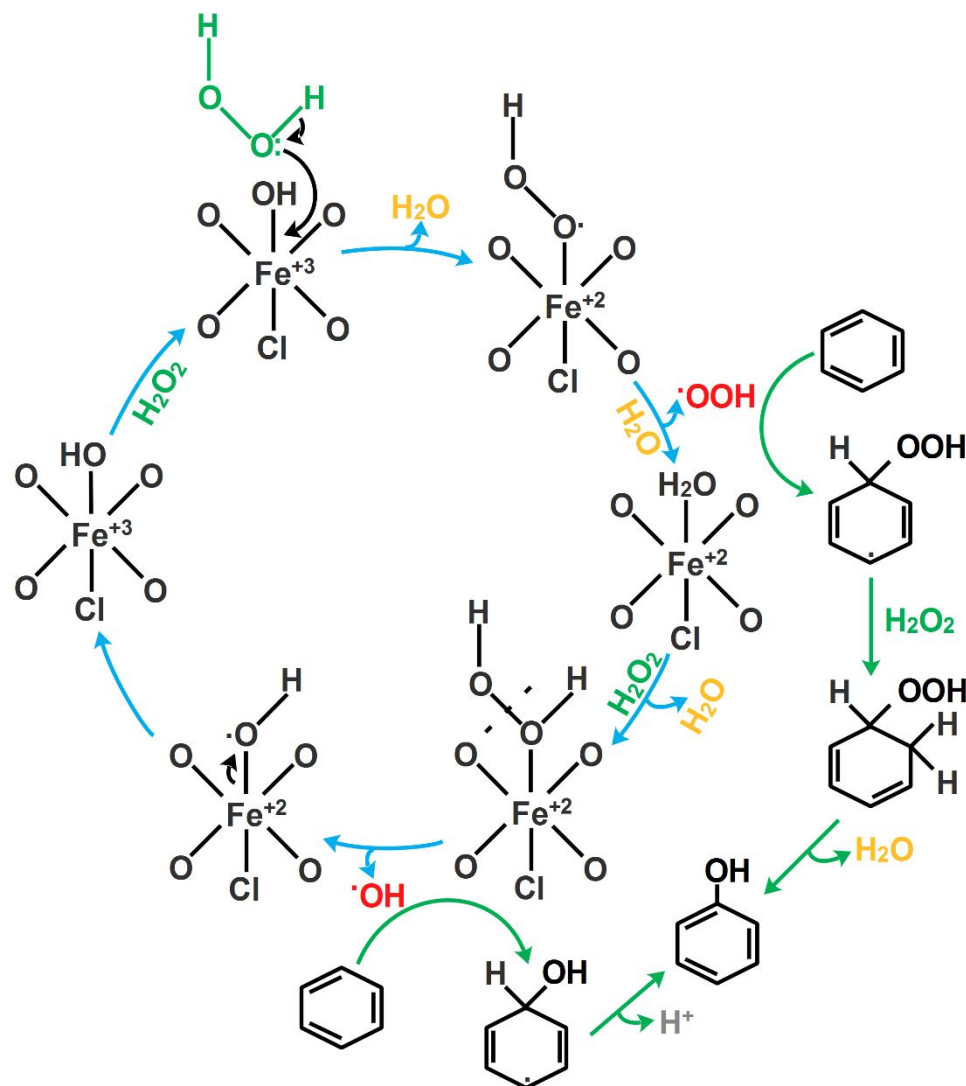
### FeOCl recovery and reuse

To check out the durability of the FeOCl in benzene hydroxylation, several experiments were carried out using the recovered FeOCl using the same employed conditions. FeOCl was recovered by centrifugation after each catalytic run, washed with ethanol and then dried at 120°C for 6 h.

1  
2  
3 The obtained results manifest that there is only a negligible decrease in the phenol yield after the  
4 fourth run using FeOCl catalyst under the same condition as displayed in Table S4. Thus, it can be  
5 inferred that the employed FeOCl is able to endure the harsh reaction condition of the benzene  
6 hydroxylation reaction. The phase of the recovered catalyst was investigated using XRD analysis  
7 to make sure that the catalyst did not suffer from any phase transformation during the catalytic  
8 activity and the obtained XRD patterns of the fresh and recovered catalyst is displayed in Figure  
9 S3. The obtained XRD pattern of the recovered catalyst reveals that did not undergo any phase  
10 transformation during benzene hydroxylation, however, a slight decrease in the peaks intensity  
11 was only observed.  
12  
13  
14  
15  
16  
17  
18  
19  
20  
21  
22  
23

### 24 **Insight into the mechanism of benzene hydroxylation using FeOCl**

25  
26  
27 As mentioned previously the efficacy of FeOCl in benzene hydroxylation is attributed to  
28 the unique ability of FeOCl for the production of a high amount of hydroxyl radicals in a short  
29 period of time and this process takes place via several successive steps. First, the facile self-redox  
30 potential of FeOCl fosters the prompt reduction of Fe<sup>3+</sup> to Fe<sup>2+</sup> upon the reaction with hydrogen  
31 peroxide (Scheme 1), which finally produces hydroperoxyl radical.<sup>45</sup> The generated Fe<sup>2+</sup> then  
32 reacts with hydrogen peroxide to produce hydroxyl radical and to eventually accomplish the redox  
33 cycle comprising the Fe<sup>2+</sup>/ Fe<sup>3+</sup> pair. It is to be noted that this redox cycle is deemed the essence  
34 of the homogeneous Fenton reaction where the reduction ferric ions to ferrous ions is the rate  
35 determining step that controls the reaction rate.<sup>46</sup>  
36  
37  
38  
39  
40  
41  
42  
43  
44  
45  
46  
47  
48  
49  
50  
51  
52  
53  
54  
55  
56  
57  
58  
59  
60



**Scheme 1.** Illustration of benzene hydroxylation mechanism using FeOCl

Moreover, FeOCl enhances the production of hydroxyl radicals by dodging the undesirable oxidation of Fe<sup>2+</sup> to Fe<sup>4+</sup>. It has been reported that Fe<sup>4+</sup> could be formed as a result of the reaction of hydrogen peroxide and Fe<sup>2+</sup> without producing hydroxyl radicals and thus this reaction was considered unfavorable.<sup>47</sup> It should be mentioned that the existence of such reaction is reason that lies behind the inefficiency of a homogeneous Fenton catalyst at neutral pH. Dodging such undesirable pathway directs the reaction between hydrogen peroxide and Fe<sup>2+</sup> toward the production of hydroxyl radicals. The exposure of a huge number of unsaturated iron atoms over

1  
2  
3 the plane (020) is considered the driving force for the prompt reduction of  $\text{Fe}^{3+}$  to  $\text{Fe}^{2+}$  and dodging  
4 the undesirable oxidation of  $\text{Fe}^{2+}$  to  $\text{Fe}^{4+}$  to produce hydroxyl radical.<sup>45</sup> These exposed atoms can  
5  
6 act as an active center for the activation of hydrogen peroxide. Moreover, the coordination of  
7  
8 chlorine and oxygen boosts the reduction potential of the exposed iron atoms. Thus, electron  
9  
10 transfer takes place more efficiently from the hydrogen peroxide molecule during the reduction of  
11  
12  $\text{Fe}^{3+}$  to  $\text{Fe}^{2+}$  and homolytic cleavage of hydrogen peroxide.<sup>48</sup>  
13  
14  
15  
16

17  
18 In particular, the produced hydroxyl radical attack the benzene molecule to produce  
19  
20 benzene-OH-adduct as presented in scheme 1. Next, benzene-OH-adduct produces phenol by  
21  
22 losing hydrogen. On another hand, the generated hydroperoxyl radicals may also attack the  
23  
24 benzene molecule to produce benzene-OOH-adduct. Thereafter, hydrogen peroxide reacts with the  
25  
26 benzene-OOH-adduct that gives rise to a benzene-hydrogen-transferred OOH-adduct, which  
27  
28 finally produces phenol by losing water molecule.<sup>49-50</sup>  
29  
30  
31

## 32 **CONCLUSIONS**

33  
34  
35 In conclusion, selective hydroxylation of benzene to produce phenol with a high phenol  
36  
37 yield (43.5%) and high selectivity (100%) has been fulfilled after only 4h of hydroxylation using  
38  
39  $\text{FeOCl}$  in the presence of hydrogen peroxide as an oxidant. The exposure of a huge number of  
40  
41 unsaturated iron atoms over the polar surface of  $\text{FeOCl}$  is considered the driving force for the  
42  
43 prompt reduction of  $\text{Fe}^{3+}$  to  $\text{Fe}^{2+}$  and dodging the undesirable oxidation of  $\text{Fe}^{2+}$  to  $\text{Fe}^{4+}$  to produce  
44  
45 considerable amount of hydroxyl radicals. The present work offers a felicitous strategy that can be  
46  
47 an alternative for conventional processes concerned with the selective hydroxylation of benzene.  
48  
49  
50

## 51 **ASSOCIATED CONTENT**

The Supporting Information is available free of charge on the ASC Publications website. Effects of reaction conditions on the selectivity and yield of phenol. Effects of reaction conditions on the selectivity of *p*-benzoquinone. Comparison between phenol selectivity and *p*-benzoquinone selectivity. Hydrogen peroxide efficiency. Comparison of catalytic activities with other catalysts for benzene hydroxylation. Reusability of FeOCl in benzene hydroxylation. XRD pattern of fresh and recovered catalyst.

## REFERENCES

- (1) Schmidt, R. J., Industrial catalytic processes—phenol production. *Appl. Catal., A* **2005**, *280*, 89-103.
- (2) Yadav, G. D.; Asthana, N. S., Selective decomposition of cumene hydroperoxide into phenol and acetone by a novel cesium substituted heteropolyacid on clay. *Appl. Catal., A* **2003**, *244*, 341-357.
- (3) Zhang, P.; Gong, Y.; Li, H.; Chen, Z.; Wang, Y., Selective oxidation of benzene to phenol by FeCl<sub>3</sub>/mpg-C<sub>3</sub>N<sub>4</sub> hybrids. *RSC Adv.* **2013**, *3*, 5121-5126.
- (4) Pirutko, L.; Chernyavsky, V.; Uriarte, A.; Panov, G., Oxidation of benzene to phenol by nitrous oxide: Activity of iron in zeolite matrices of various composition. *Appl. Catal., A* **2002**, *227*, 143-157.
- (5) Ye, X.; Cui, Y.; Wang, X., Ferrocene-Modified Carbon Nitride for Direct Oxidation of Benzene to Phenol with Visible Light. *ChemSusChem* **2014**, *7*, 738-742.
- (6) Luo, G.; Lv, X.; Wang, X.; Yan, S.; Gao, X.; Xu, J.; Ma, H.; Jiao, Y.; Li, F.; Chen, J., Direct hydroxylation of benzene to phenol with molecular oxygen over vanadium oxide nanospheres and study of its mechanism. *RSC Adv.* **2015**, *5*, 94164-94170.
- (7) Shul'pin, G. B.; Kozlov, Y. N.; Shul'pina, L. S.; Carvalho, W. A.; Mandelli, D., Oxidation reactions catalyzed by osmium compounds. Part 4. Highly efficient oxidation of hydrocarbons and alcohols including glycerol by the H<sub>2</sub>O<sub>2</sub>/Os<sup>3</sup>(CO)<sub>12</sub>/pyridine reagent. *RSC Adv.* **2013**, *3*, 15065-15074.
- (8) Niwa, S.-i.; Eswaramoorthy, M.; Nair, J.; Raj, A.; Itoh, N.; Shoji, H.; Namba, T.; Mizukami, F., A one-step conversion of benzene to phenol with a palladium membrane. *Science* **2002**, *295*, 105-107.
- (9) Balducci, L.; Bianchi, D.; Bortolo, R.; D'Aloisio, R.; Ricci, M.; Tassinari, R.; Ungarelli, R., Direct oxidation of benzene to phenol with hydrogen peroxide over a modified titanium silicalite. *Angew. Chem. Int. Ed.* **2003**, *115*, 5087-5090.
- (10) Wen, G.; Wu, S.; Li, B.; Dai, C.; Su, D. S., Active sites and mechanisms for direct oxidation of benzene to phenol over carbon catalysts. *Angew. Chem. Int. Ed. International Edition* **2015**, *54*, 4105-4109.
- (11) Yang, J.-H.; Sun, G.; Gao, Y.; Zhao, H.; Tang, P.; Tan, J.; Lu, A.-H.; Ma, D., Direct catalytic oxidation of benzene to phenol over metal-free graphene-based catalyst. *Energ. Environ. Sci.* **2013**, *6*, 793-798.

- 1  
2  
3 (12) Jiaquan, X.; Huihui, L.; Ruiguang, Y.; Guiying, L.; Changwei, H., Hydroxylation of  
4 benzene by activated carbon catalyst. *Chin. J. Catal.* **2012**, *33*, 1622-1630.
- 5 (13) Chen, C.-h.; Xu, J.-q.; Jin, M.-m.; Li, G.-y.; Hu, C.-w., Direct synthesis of phenol from  
6 benzene on an activated carbon catalyst treated with nitric acid. *Chin. J. Chem. Phys.* **2011**, *24*,  
7 358.
- 8 (14) Zhong, Y.; Li, G.; Zhu, L.; Yan, Y.; Wu, G.; Hu, C., Low temperature hydroxylation of  
9 benzene to phenol by hydrogen peroxide over Fe/activated carbon catalyst. *J. Mol. Catal. A Chem.*  
10 **2007**, *272*, 169-173.
- 11 (15) Zhong, Y.; Li, G.; Zhu, L.; Tang, D.; Hu, C., Direct catalytic hydroxylation of several  
12 typical aromatic compounds over Fe/activated carbon catalyst. *Chem. J. Chinese U.* **2007**, *28*,  
13 1570.
- 14 (16) Jian, M.; Zhu, L.; Wang, J.; Zhang, J.; Li, G.; Hu, C., Sodium metavanadate catalyzed  
15 direct hydroxylation of benzene to phenol with hydrogen peroxide in acetonitrile medium. *J. Mol.*  
16 *Catal. A Chem.* **2006**, *253*, 1-7.
- 17 (17) Zhang, J.; Tang, Y.; Xie, J.-q.; Song, Z.-r.; Wang, L.; Hu, C.-w., The catalytic oxidation of  
18 phenol with H<sub>2</sub>O<sub>2</sub> by metalloporphyrins as peroxidase mimics. *React. Kinet. Catal. L* **2005**, *85*,  
19 269-276.
- 20 (18) Zhang, J.; Tang, Y.; Xie, J.-Q.; Li, J.-Z.; Zeng, W.; Hu, C.-W., Study on phenol oxidation  
21 with H<sub>2</sub>O<sub>2</sub>. *J. Serb. Chem. Soc.* **2005**, *70*, 1137-1146.
- 22 (19) Zhang, J.; Tang, Y.; Li, G.; Hu, C., Room temperature direct oxidation of benzene to phenol  
23 using hydrogen peroxide in the presence of vanadium-substituted heteropolymolybdates. *Appl.*  
24 *Catal., A* **2005**, *278*, 251-261.
- 25 (20) Zhang, J.; Tang, Y.; Luo, Q.; Jian, M.; Hu, C., Study on the synthesis of heteropoly acids  
26 containing different amount of V and Mo and their catalytic performance for the direct  
27 hydroxylation of benzene to phenol. *Chinese J. Inorg. Chem.* **2004**, *20*, 935-940.
- 28 (21) Wang, C.; Hu, L.; Wang, M.; Yue, B.; He, H., Cerium promoted V-g-C<sub>3</sub>N<sub>4</sub> as highly  
29 efficient heterogeneous catalysts for the direct benzene hydroxylation. *R. Soc. open sci.* **2018**, *5*,  
30 180371-180380.
- 31 (22) Hu, L.; Wang, C.; Yue, B.; Chen, X.; He, H., Vanadium-containing mesoporous carbon  
32 and mesoporous carbon nanoparticles as catalysts for benzene hydroxylation reaction. *Mater.*  
33 *Today Commun.* **2017**, *11*, 61-67.
- 34 (23) Wang, Y.; Zhang, T.; Li, B.; Jiang, S.; Sheng, L., Synthesis, characterization,  
35 electrochemical properties and catalytic reactivity of N-heterocyclic carbene-containing diiron  
36 complexes. *RSC Adv.* **2015**, *5*, 29022-29031.
- 37 (24) Wu, L.; Zhong, W.; Xu, B.; Wei, Z.; Liu, X., Synthesis and characterization of copper (II)  
38 complexes with multidentate ligands as catalysts for the direct hydroxylation of benzene to phenol.  
39 *Dalton Trans.* **2015**, *44*, 8013-8020.
- 40 (25) Wen, N.; Xu, F.; Feng, Y.; Du, S., A new cumulene diiron complex related to the active  
41 site of Fe-only hydrogenases and its phosphine substituted derivatives: Synthesis, electrochemistry  
42 and structural characterization. *J. Inorg. Biochem.* **2011**, *105*, 1123-1130.
- 43 (26) Wang, D.; Wang, M.; Li, Z., Fe-based metal-organic frameworks for highly selective  
44 photocatalytic benzene hydroxylation to phenol. *Acs Catal.* **2015**, *5*, 6852-6857.
- 45 (27) Jourshabani, M.; Badiei, A.; Shariatnia, Z.; Lashgari, N.; Mohammadi Ziarani, G., Fe-  
46 supported SBA-16 type cagelike mesoporous silica with enhanced catalytic activity for direct  
47 hydroxylation of benzene to phenol. *Ind. Eng. Chem. Res.* **2016**, *55*, 3900-3908.
- 48  
49  
50  
51  
52  
53  
54  
55  
56  
57  
58  
59  
60

- 1  
2  
3 (28) Baykan, D.; Oztas, N. A., Synthesis of iron orthophosphate catalysts by solution and  
4 solution combustion methods for the hydroxylation of benzene to phenol. *Mater. Res. Bull.* **2015**,  
5 *64*, 294-300.
- 6 (29) Carneiro, L.; Silva, A. R., Selective direct hydroxylation of benzene to phenol with  
7 hydrogen peroxide by iron and vanadyl based homogeneous and heterogeneous catalysts. *Catal.*  
8 *Sci. Technol.* **2016**, *6*, 8166-8176.
- 9 (30) Al-Sabagh, A. M.; Yehia, F. Z.; Eshaq, G.; ElMetwally, A. E., Eclectic hydroxylation of  
10 benzene to phenol using ferrites of Fe and Zn as durable and magnetically retrievable catalysts.  
11 *ACS Sustain. Chem. Eng.* **2017**, *5*, 4811-4819.
- 12 (31) Herber, R.; Cassell, R., Synthesis, hyperfine interactions, and lattice dynamics of the  
13 intercalation compound (FeOCl (Kryptofix-21) 1/18. *Inorg. Chem.* **1982**, *21*, 3713-3716.
- 14 (32) Jarrige, I.; Cai, Y.; Shieh, S.; Ishii, H.; Hiraoka, N.; Karna, S.; Li, W.-H., Charge transfer  
15 in FeOCl intercalation compounds and its pressure dependence: An x-ray spectroscopic study.  
16 *Phys. Rev. B* **2010**, *82*, 165121.
- 17 (33) Hwang, S.; Li, W.-H.; Lee, K.; Lynn, J.; Wu, C.-G., Spiral magnetic structure of Fe in Van  
18 der Waals gapped FeOCl and polyaniline-intercalated FeOCl. *Phys. Rev. B* **2000**, *62*, 14157.
- 19 (34) Yang, X.-j.; Xu, X.-m.; Xu, J.; Han, Y.-f., Iron oxychloride (FeOCl): an efficient Fenton-  
20 like catalyst for producing hydroxyl radicals in degradation of organic contaminants. *J. Am. Chem.*  
21 *Soc.* **2013**, *135*, 16058-16061.
- 22 (35) Borah, P.; Datta, A.; Nguyen, K. T.; Zhao, Y., VOPO 4· 2H 2 O encapsulated in graphene  
23 oxide as a heterogeneous catalyst for selective hydroxylation of benzene to phenol. *Green Chem.*  
24 **2016**, *18*, 397-401.
- 25 (36) ElShafei, G. M. S.; Al-Sabagh, A. M.; Yehia, F. Z.; Philip, C. A.; Moussa, N. A.; Eshaq,  
26 G.; ElMetwally, A. E., Metal oxychlorides as robust heterogeneous Fenton catalysts for the  
27 sonophotocatalytic degradation of 2-nitrophenol. *Appl. Catal. B Environ.* **2018**, *224*, 681-691.
- 28 (37) ElMetwally, A. E.; Eshaq, G.; Al-Sabagh, A. M.; Yehia, F. Z.; Philip, C. A.; Moussa, N.  
29 A.; ElShafei, G. M. S., Insight into heterogeneous Fenton-sonophotocatalytic degradation of  
30 nitrobenzene using metal oxychlorides. *Sep. Purif. Technol.* **2019**, *210*, 452-462.
- 31 (38) Eggleston, C. M.; Stack, A. G.; Rosso, K. M.; Higgins, S. R.; Bice, A. M.; Boese, S. W.;  
32 Pribyl, R. D.; Nichols, J. J., The structure of hematite ( $\alpha$ -Fe<sub>2</sub>O<sub>3</sub>)(001) surfaces in aqueous media:  
33 scanning tunneling microscopy and resonant tunneling calculations of coexisting O and Fe  
34 terminations. *Geochim. Cosmochim. Acta* **2003**, *67*, 985-1000.
- 35 (39) Pignatello, J. J.; Oliveros, E.; MacKay, A., Advanced oxidation processes for organic  
36 contaminant destruction based on the Fenton reaction and related chemistry. *Crit. Rev. Environ.*  
37 *Sci. Technol.* **2006**, *36*, 1-84.
- 38 (40) Buxton, G. V.; Greenstock, C. L.; Helman, W. P.; Ross, A. B., Critical review of rate  
39 constants for reactions of hydrated electrons, hydrogen atoms and hydroxyl radicals ( $\cdot$ OH/ $\cdot$ O $^-$  in  
40 aqueous solution. *J. Phys. Chem. Ref. Data* **1988**, *17*, 513-886.
- 41 (41) Mehrdad, A.; Hashemzadeh, R., Ultrasonic degradation of Rhodamine B in the presence  
42 of hydrogen peroxide and some metal oxide. *Ultrason. Sonochem.* **2010**, *17*, 168-172.
- 43 (42) Yehia, F.; Eshaq, G.; ElMetwally, A., Role of surface modification of some metal oxides  
44 with amino acids in upgrading the sonocatalytic degradation of nitrobenzene. *Desalin. Water*  
45 *Treat.* **2015**, *56*, 2160-2167.
- 46 (43) Yehia, F. Z.; Eshaq, G.; ElMetwally, A. E., Enhancement of the working pH range for  
47 degradation of p-nitrophenol using Fe<sup>2+</sup>-aspartate and Fe<sup>2+</sup>-glutamate complexes as modified  
48 Fenton reagents. *Egypt. J. Pet.* **2016**, *25*, 239-245.
- 49  
50  
51  
52  
53  
54  
55  
56  
57  
58  
59  
60

- 1  
2  
3 (44) Karimi, L.; Zohoori, S.; Yazdanshenas, M. E., Photocatalytic degradation of azo dyes in  
4 aqueous solutions under UV irradiation using nano-strontium titanate as the nanophotocatalyst. *J.*  
5 *Saudi Chem. Soc.* **2014**, *18*, 581-588.
- 6 (45) Sun, M.; Chu, C.; Geng, F.; Lu, X.; Qu, J.; Crittenden, J.; Elimelech, M.; Kim, J.-H.,  
7 Reinventing Fenton Chemistry: Iron Oxochloride Nanosheet for pH-Insensitive H<sub>2</sub>O<sub>2</sub> Activation.  
8 *Environ. Sci. Technol. Lett.* **2018**, *5*, 186-191.
- 9 (46) Kim, B. J.; Lee, D. U.; Wu, J.; Higgins, D.; Yu, A.; Chen, Z., Iron-and nitrogen-  
10 functionalized graphene nanosheet and nanoshell composites as a highly active electrocatalyst for  
11 oxygen reduction reaction. *J. Phys. Chem. C* **2013**, *117*, 26501-26508.
- 12 (47) Koppenol, W.; Liebman, J. F., The oxidizing nature of the hydroxyl radical. A comparison  
13 with the ferryl ion (FeO<sup>2+</sup>). *J. Phys. Chem.* **1984**, *88*, 99-101.
- 14 (48) Li, H.; Shang, J.; Yang, Z.; Shen, W.; Ai, Z.; Zhang, L., Oxygen vacancy associated surface  
15 Fenton chemistry: Surface structure dependent hydroxyl radicals generation and substrate  
16 dependent reactivity. *Environ. Sci. Technol.* **2017**, *51*, 5685-5694.
- 17 (49) Hirose, K.; Ohkubo, K.; Fukuzumi, S., Catalytic Hydroxylation of Benzene to Phenol by  
18 Dioxygen with an NADH Analogue. *Chem. Eur. J.* **2016**, *22*, 12904-12909.
- 19 (50) Yamada, M.; Karlin, K. D.; Fukuzumi, S., One-step selective hydroxylation of benzene to  
20 phenol with hydrogen peroxide catalysed by copper complexes incorporated into mesoporous  
21 silica–alumina. *Chem. Sci.* **2016**, *7*, 2856-2863.
- 22  
23  
24  
25  
26  
27  
28  
29  
30  
31  
32  
33  
34  
35  
36  
37  
38  
39  
40  
41  
42  
43  
44  
45  
46  
47  
48  
49  
50  
51  
52  
53  
54  
55  
56  
57  
58  
59  
60



1  
2  
3  
4  
5  
6  
7  
8  
9  
10  
11  
12  
13  
14  
15  
16  
17  
18  
19  
20  
21  
22  
23  
24  
25  
26  
27  
28  
29  
30  
31  
32  
33  
34  
35  
36  
37  
38  
39  
40  
41  
42  
43  
44  
45  
46  
47  
48  
49  
50  
51  
52  
53  
54  
55  
56  
57  
58  
59  
60

